Colloids and Surfaces A: Physicochemical and Engineering Aspects 630 (2021) 127663

Contents lists available at ScienceDirect

Colloids and Surfaces A: Physicochemical and Engineering Aspects

journal homepage: www.elsevier.com/locate/colsurfa

Engineering and development of model lipid membranes mimicking the HeLa cell membrane

Adrià Botet-Carreras [a,b], M. Teresa Montero [a,b], Jesús Sot [c], Òscar Domènech [a,b,*], Jordi H. Borrell [a,b]

[a] Secció de Fisicoquímica, Facultat de Farmàcia i Ciències de l'Alimentació, Spain
[b] Institute of Nanoscience and Nanotechnology (IN2UB), Universitat de Barcelona (UB), 08028 Barcelona, Catalonia, Spain
[c] Instituto Biofisika (CSIC-UPV/HEU) Campus Universitario, 48940 Leioa, Basque Country, Spain

HIGHLIGHTS

- A lipid bilayer mimicking the HeLa membrane cell is characterised.
- HeLa-mimicking liposomes show phase coexistence at room temperature.
- Laterally segregated domains are not observed by AFM in Supported Lipid Bilayers.
- Fusion of liposomes changes Young's modulus of HeLa-mimicking bilayers.
- POPC:DOTAP and POPC:CHOL:DOTAP liposomes fusing process with HeLa-mimicking bilayers is characterised by FRET fluorescence.
- Changes in liposomes microviscosity and fluorescence lifetime corroborate the fusion process.

GRAPHICAL ABSTRACT

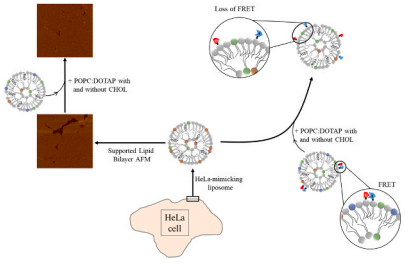

ARTICLE INFO

Keywords:
HeLa lipid bilayer models
Atomic force microscopy (AFM)
Förster resonance energy transfer (FRET)
Microviscosity

ABSTRACT

Cells are complex systems whose interaction with nanocarriers, i.e., liposomes, are continuously under investigation to improve drug uptake. Model membranes can facilitate the understanding of the processes involved in fusion or endocytosis. In this work, we engineered two different lipid model membranes, vesicles and supported lipid bilayers (SLBs), mimicking the lipid composition of the HeLa cell plasma membrane. We characterized the model using atomic force microscopy (AFM) and fluorescence. We found that liposomes formed with four lipid components mimicking the HeLa cell bilayer show a liquid ordered fluid nature between 13 °C and 34 °C and yield featureless SLBs onto mica. We evaluated the fusion between the model and liposomes positively charged with and without cholesterol by AFM-based force spectroscopy and fluorescence techniques, such as Förster resonance energy transfer, fluorescence lifetime decay and fluorescence anisotropy. The results indicated a primary electrostatic interaction between the HeLa bilayer model and the liposomes. It was also confirmed the well-known fact that cholesterol enhances the fusion process with the engineered HeLa bilayer. All results support the usefulness of the engineered model in the rationale design of liposomes for drug delivery.

* Corresponding author at: Secció de Fisicoquímica, Facultat de Farmàcia i Ciències de l'Alimentació, Av. Joan XXIII 27-31, 08028 Barcelona, Spain.
E-mail address: odomenech@ub.edu (Ò. Domènech).

https://doi.org/10.1016/j.colsurfa.2021.127663
Received 23 August 2021; Received in revised form 28 September 2021; Accepted 29 September 2021
Available online 2 October 2021

1. Introduction

One of the most widely researched phenomena in biophysics is to understand the interaction of macromolecules with cells as it is the first step in several biophysical/biochemical processes, such as DNA transfection and drug delivery [1–3]. The complexity of cell membranes, i.e., lipid heterogeneity as well as the adsorbed or embedded membrane proteins, is a barrier for the interpretation of the physicochemical properties governing these processes. To overcome this, simplified model membrane systems are mandatory to unveil the nature of the interaction with cell membranes. The most common and well-known model membrane systems are monolayers, liposomes and membranes formed onto solid substrates. All these systems mimic the properties of cell membranes such as the lipid composition, lipid curvature, domains and rafts, depending on the system and the combination of compounds chosen as well as on the physicochemical properties of interest.

Transfecting material into cells has been a wide field of study, with liposomes playing a significant role. Liposomes, referred to as drug delivery systems, are an excellent model for mimicking cell membranes and experimentally testing the conditions that favour the internalisation of the encapsulated drug or carrying molecules by eukaryotic cells or bacteria. The extensive literature on liposome-based drug-delivery systems has been enriched by the development of surface functionalisation and modifications designed to achieve selectivity as well as to overcome removal by the reticuloendothelial system and circumvent the immune response system among other challenges [4]. However, it is not fully understood if liposomes fuse with the cell membrane or if they are endocytosed and subsequently degraded liberating their content into the cytoplasm. Despite the many years of extensive research into these processes (fusion and fission) at the molecular level, research in this field continues to expand and is of paramount importance for understanding the various biological processes in which fusion plays a leading role.

The fusion of two membranes, e.g., a cell membrane with a vesicle, is a complex process that involves many factors, but can be improved by engineering appropriate vesicles. For example, the addition of SNARE (Soluble NSF Attachment Protein Receptor) proteins promotes fusion and leads to pore opening in the cell membrane to release the liposome content [5]. The presence of lipids promoting the negative curvature of the vesicle, such as phosphatidylethanolamine (PE)[6,7], also facilitates the fusion process after adsorption of the two bilayers possibly through the emergence of hexagonal phases (H_{II}) at the intermediate stages of the fusion process. It is also well known that cholesterol plays a key role in the fusion process as well as the cationic lipid 1,2-dioleoyl-3-trimethylammonium-propane (DOTAP), particularly in DNA transfection.

One of our current research projects is the engineering of liposomes for transporting proteins and genes into HeLa cell membranes [8]. Our ultimate goal is to test the ability of a liposome-based nanocarrier that can transfect proteins or genes to repair defects in cell membranes caused by the malfunction of proteins that are either absent due to DNA mutation or not well folded and presenting a non-functional conformation. Such defects are the main cause of many unrelated diseases that have severe consequences [9–11]. In a previous work [12], we developed and characterised an artificial monolayer lipid membrane that mimicked the HeLa lipid membrane. This lipid model had four components: 1-palmitoyl-2-oleoyl-*sn*-glycero-3-phosphatidylcholine (POPC), 1-palmitoyl-2-oleoyl-*sn*-glycero-3-phosphoethanolamine (POPE), 1-palmitoyl-2-oleoyl-*sn*-glycero-3-phospho-L-serine (POPS) and cholesterol (CHOL).

In the present work, we present data extending the characterisation of HeLa lipid vesicles and supported lipid bilayers (SLBs). The physicochemical characterisation of both models and how they behave when investigating the fusion with engineered liposomes may be relevant to interpret the events occurring in the interaction between these liposomes and living cells. Thus, in the present paper we have evaluated these two HeLa lipid models in their fusion with liposomes containing the cationic lipid DOTAP with or without cholesterol. For the phase characterisation of the vesicle HeLa lipid bilayer model we used fluorescence spectroscopy applying a ratiometric parameter, the red/blue intensity ratio (RBIR), of the 1-formyl-6-(N-cyclohexyl) aminopyrene (PA) probe [13] alongside conventional fluorescence anisotropy. These information provided by the latter measurements indicated the changes in viscosity of the HeLa lipid membrane model after fusion with POPC:DOTAP or POPC:CHOL:DOTAP liposomes. Furthermore, exploiting the Förster resonance energy transfer (FRET) technique, we examined the fusion process between liposomes mimicking the HeLa lipid membrane and liposomes containing two fluorescent probes, nitrobenzoxadiazole (NBD) and rhodamine (Rh). Finally, fluorescence lifetime decay measurements were used to corroborate the interaction between the engineered liposomes and the engineered model. We also investigated the topographic characteristics and viscoelastic properties (Young's modulus) of SLBs trough atomic force microscopy (AFM)-based force spectroscopy analysis in the presence and absence of POPC:DOTAP or POPC:CHOL:DOTAP liposomes.

2. Experimental section

2.1. Materials

1-palmitoyl-2-oleoyl-*sn*-glycero-3-phosphatidylcholine (POPC), 1-palmitoyl-2-oleoyl-*sn*-glycero-3-phosphoethanolamine (POPE), 1-palmitoyl-2-oleoyl-*sn*-glycero-3-phospho -L-serine (POPS), 1,2-dioleoyl-3-trimethylammonium-propane (chloride salt) (DOTAP), cholesterol (CHOL), 1,2-dioleoyl-*sn*-glycero-3-phosphoethanolamine-N-(lissamine rhodamine B sulfonyl)(ammonium salt) (Rh-PE) and 1,2-dioleoyl-*sn*-glycero-3-phosphoethanolamine-N-(7-nitro-2–1,3-benzoxadiazol-4-yl) (ammonium salt) (NBD-PE) were purchased from Avanti Polar Lipids (Alabaster, AL, USA). The lipophilic fluorescent probe 1-formyl-6-(N-cyclohexyl) aminopyrene (PA) was synthetized as previously described [14] and was a kind gift from Andrey Klymchenko (CNRS, Illkirch, France). 1,6-diphenylhexatriene (DPH) and 1-(4-trimethylammoniumphenyl)−6-phenyl-1,3,5-hexatriene (TMA-DPH) were purchased from Invitrogen (Life Technologies Ltd., Paisley, UK). All the other chemicals were acquired from Sigma-Aldrich (St. Louis, MO, USA) and used as received. Round muscovite mica discs, 9.5 mm diameter and 0.15–0.21 mm thickness, were purchased from Electron Microscopy Sciences (Hatfield, PA, USA). The lipids were dissolved in a chloroform:methanol (2:1, v/v) solution to obtain a final concentration of 1 mg mL^{-1}. These solutions were used to obtain the mixtures POPC:POPE:POPS:CHOL (0.29:0.31:0.06:0.34, mol/mol/mol/mol) [15–18], and is referred through the text as HeLa-mimicking mixture (either HeLa liposomes or HeLa SLBs), POPC:DOTAP (0.80:0.20, mol/mol) and POPC:CHOL:DOTAP (0.65:0.15:0.20, mol/mol/mol).

2.2. Liposome preparation

Chloroform:methanol (2:1, v/v) solution containing the appropriate amount of lipids was placed in a glass balloon flask and dried in a rotary evaporator at room temperature, protected from light. The resulting thin film was kept under high vacuum overnight to remove any traces of organic solvent. Multilamellar liposomes (MLVs) were obtained by redispersion of the thin film in 10 mM Tris·HCl, 150 mM NaCl buffer, pH 7.4. Large unilamellar vesicles (LUVs) were obtained by extrusion through polycarbonate membranes with a pore size of 100 nm, using an Avanti®Mini-extruder (Avanti Polar Lipids Inc., Alabaster, AL, USA). The mean particle size and polydispersity values of the liposomes were measured by dynamic light scattering with a Zetasizer Nano S (Malvern Instruments, UK). To assess the effective surface electrical charge, electrophoretic mobility was determined with a Zetasizer Nano ZS90 (Malvern Instruments, UK). Each sample was measured at least three times.

2.3. Supported lipid bilayers

Supported lipid bilayers (SLBs) were obtained through the vesicle fusion method, as previously described in detail [19]. Briefly, a round Teflon disc was glued to a steel disc and a mica disc was mounted on top of the Teflon disc. 50 μL of 250 μM HeLa-mimicking liposomes were deposited onto freshly cleaved mica surface. Liposome suspension was incubated for 2 h at 40 °C, temperature over the transition temperature of any individual pure phospholipid used in the study. To prevent sample evaporation, the sample was enclosed in a small petri dish inside a bigger petri dish with some water at the bottom used as a reservoir. The big petri dish was then sealed with Teflon ribbon and placed inside an oven (Termaks AS, Bergen, Norway) with temperature control of ±0.2 °C. After incubation, non-adsorbed liposomes were removed by gently rinsing samples with buffer and letting them stabilize overnight at room temperature.

2.4. AFM imaging and force spectroscopy

AFM images and force spectroscopy measurements were performed with a Nanoscope IV from Digital Instruments (Bruker, AXS Co., Madison, WI, USA), equipped with a 15 μm piezoelectric scanner. Samples were directly mounted on the top of the AFM scanner and let to stabilize for no less than 30 min before beginning the scan. Temperature and humidity were maintained at 24 °C and 60%, respectively. SLB images were obtained using V-shaped silicon nitride cantilevers (MSNL-10, Bruker, USA) with a nominal spring constant of 30 pN nm^{-1}, in liquid and in intermittent contact mode. During the experiments, the force applied to the samples was kept as low as possible to minimize sample damage. All the images were processed using NanoScope® analysis software (Bruker, AXS Co., Madison, WI, USA).

When performing force spectroscopy experiments in liquid, individual spring constants (k_c) were calibrated using the thermal noise method, after the photodetector optical sensitivity (V nm^{-1}) had been correctly determined by measuring it at high voltages. Applied forces, F, are given by $F = k_c \times \delta$, where δ stands for the cantilever deflection. Mechanical properties were measured by recording arrays of 32 × 32 force curves, using a maximum force of 0.5–1 nN to avoid sample damage, and approach and retract speeds of 1.0 μm/s.

2.5. Young's modulus

Young's modulus is a physicochemical parameter that evaluates the stiffness of a sample, providing information on how difficult is to deform the sample in the direction of the force applied. In the present study, we have calculated the Young's modulus by means of AFM [20] as a physicochemical parameter that informs on the cohesive force between the lipids forming the lipid bilayer [21]. The Young's modulus of the different samples was determined as a first approximation and with the aim of observing relative differences in its value after liposome fusion using the Hertz model. This model considers that: (i) the surface of the sample is a homogeneous, isotropic and linear elastic solid, (ii) the indenter is not deformable, and (iii) the interaction between sample and indenter is through elastic forces only. If we consider the indenter as a parabolic tip, the Young's modulus can be calculated from force-indentation curve data thus,

$$F = \frac{4\sqrt{r_{tip}}}{3} \cdot \frac{E}{1-\upsilon^2} \cdot \delta^{3/2} \quad (1)$$

where r_{tip} is the tip radius, υ the Poisson's ratio (0.5 for most biological samples) and E the Young's modulus. Tip radius values were evaluated using a reference pattern and show satisfactory matches with the values supplied by the manufacturer (2 nm).

2.6. Fluorescence experiments

2.6.1. Red/blue intensity ratio (RBIR) measurements

MLV for the RBIR measurements at 1 mM with PA were prepared, as described above, by mixing the desired lipids and PA at a molar ratio of 250:1 (lipid:PA). Samples were sonicated in a bath sonicator FB-15049 (Fisher Scientific, Waltham, MA, USA) at a temperature above the transition temperature for 10 min and finally diluted to a 0.3 mM final lipid concentration. The fluorescence spectra of the PA probe were measured at different temperatures in a QuantaMaster 40 Spectrofluorometer (Photon Technology International, Lawrenceville, N.J., USA). Emission spectra were collected between 450 and 700 nm, exciting at 430 nm for PA using a 430 nm bandpass filter to minimize detection of dispersed light. A thermal TC125 controller (Quantum Northwest, Liberty Lake, WA, USA) was used to stabilize the sample temperature. Data analysis was performed in a similar way to that used by Niko et al. [14], using the ratiometric response of the dye, i.e., calculating the integral intensity ratio of red/blue regions of the emission band (573–613 nm/500–530 nm). In order to calculate the RBIR values, the areas of the blue (500–530 nm) and red (573–613 nm) regions of the emission spectra were subtracted with PTI Felix-GT software (Photon Technology International, Lawrenceville, N.J., USA). This methodology allows distinguishing between L_o, L_α and L_β phases [13].

2.6.2. Förster resonance energy transfer (FRET) assays

Typically, FRET assays are performed on the extent of resonance energy transfer (RET) between two labelled lipids, in our case between NBD-PE and Rh-PE, as described in other publications [22]. In our experiments both probes are in the same engineered liposome and, under the fusion process with non-labelled liposomes of the HeLa-mimicking mixture, the fluorescent probes will be more diluted. Therefore, the RET signal, more precisely Rh-PE fluorescence, will not be detected while the NBD-PE signal will increase.

Liposomes for FRET assays were labelled adding 0.6% of each probe (NBD-PE and Rh-PE) to the desired liposome composition during liposome formation. Fluorescence measurements were performed in 1 mL of 10 mM Tris·HCl, 150 mM NaCl buffer, pH 7.4 containing 20 μM of fluorescent labelled liposomes. The sample was left to stabilize for 30 min at 37 °C in a dark environment before the fusion experiments started. After that period, 20 μM of unlabelled HeLa-mimicking liposomes were added to the cuvette and fluorescence of NBD at 547 nm was monitored as a function of time.

The percentage of fusion was calculated using the following equation,

$$\%Fusion = \left(\frac{F_t - F_0}{F_\infty}\right) \times 100 \quad (2)$$

where F_t is the NBD fluorescence intensity at each given time, F_0 the initial NBD fluorescence intensity and F_∞ the fluorescence intensity at infinite dilution of the fluorescent probe in liposomes. It is commonly used the addition of detergents to obtain the F_∞ value, but NBD fluorescence is affected by the local environment of the dye. It is reported that NBD fluorescence in micelles presents less fluorescence than when NBD molecules are infinite diluted [23]. More precisely $F_\infty = \alpha \cdot F_{det}$ where F_{det} is the fluorescence of NBD in micelles and α is a ratio of the real fluorescence at infinite dilution to that with detergent. In our experiments, F_{det} was experimentally determined after the rupture of the sample by TritonX-100 at a final concentration of 1% (checked by quasi-elastic light spectroscopy), and α value used was 1.79 at 37 °C [23]. Under our experimental conditions, and considering that aggregation number of TritonX-100 is between 150 and 200, after the solubilization of liposomes by the detergent we had less than 0.3 lipid molecules in each micelle, so FRET signal should be almost supressed. All experimental data were corrected from inner filter and reabsorption effects.

Fusion data can be fitted to a modified Langmuir saturation curve to evaluate the physicochemical parameters of the process as:

$$\%Fusion = A_{max}\frac{kt^b}{1+kt^b} \quad (3)$$

where A_{max} is the maximum value of fusion achieved, k the rate constant of the process and b a parameter related with the cooperativity of the process.

2.6.3. Measurement of viscosity using DPH and TMA-DPH fluorescence anisotropy

Liposome membrane fluidity can be investigated by using the decrease in fluorescence polarization of DPH or TMA-DPH. Briefly, as described elsewhere [24] liposomes were labelled using a lipid to probe molar ratio of 300. The desired DPH or TMA-DPH volume was added to a 500 μM liposome solution and incubated, protected from light, for 30 min at a temperature above the transition temperature of the lipidic mixture. Afterwards, the degree of polarization of the sample was determined measuring the fluorescence intensity parallel and perpendicular with respect to the plane of linearly polarized excitation light at 381 nm.

To calculate the microviscosity of liposomes from polarization data we follow the method previously established by Shinitzky and Barenholz [25] and recently applied by Kure and Sakai [26]. A relationship between the microviscosity (η) of the medium (the liposome membrane) and the anisotropy (r) in the steady state of a fluorescent probe dissolved in that medium can be evaluated by using the Perrin equation,

$$\frac{r_0}{r} = 1 + C(r)\frac{T\cdot\tau}{\eta} \quad (4)$$

where T is the absolute temperature, τ the excited-state lifetime of the fluorescent probe, r_0 the limiting anisotropy and $C(r)$ a parameter related to the molecular shape and the location of the transition dipoles of the rotating fluorophore at each r value. The term $C(r)\cdot T\cdot\tau$ in Eq. 4 has been experimentally determined as 0.24 Pa·s while the r_0 value for the DPH molecule is 0.362. Eq. 4 can be rearranged, as a first approximation thus,

$$\eta(Pa\cdot s) = \frac{0.24\cdot r}{0.362 - r} \quad (5)$$

To further the analysis of the physicochemical properties of liposomes used in this study, we evaluate the dependence of the viscosity on temperature. The common solvents and linear hydrocarbon chain liquids follow an exponential decay of their viscosity as a function of temperature, as described by the empirical correlation,

$$\eta = \eta_0 e^{\frac{\Delta E}{RT}} \quad (6)$$

where η_0 is lowest viscosity value of the liquid, R the gas constant and ΔE the activation energy that accounts for the minimum energy value required for the fluid to flow. In our case, where the liquid is confined in the form of a liposome membrane this energy could be considered as the minimum energy to diffuse or flow. This magnitude can be either understood as an estimation of the minimum energy required to trigger the first events occurring in fusion between different bilayers or extension of liposomes onto surfaces. Therefore, the higher this energy is the lower would be the probability of fusion between lipid membranes.

FRET assays, DPH and TMA-DPH anisotropy measurements were performed using an SLM-Aminco 8100 spectrofluorometer equipped with a jacketed cuvette holder. Temperature (±0.2 °C) was controlled using a circulating bath (Haake K20, Germany). The excitation and emission slit widths were 4 and 4 nm, and 8 and 8 nm, respectively.

2.6.4. Lifetime fluorescence decay

NBD-PE and Rh-PE fluorescence lifetime decay in liposomes were determined with a PTI EasyLife LED fluorescence lifetime instrument (Horiba Ltd., UK) using 460 nm excitation pulses while monitoring the emission through a band pass filter of 530 nm. Samples of 1 mL at 20 μM of lipid were analysed with an integration time of 0.3 s and with an average of 3 runs. Ludox® solution was used to correct the instrument response factor (IRF). All data were processed with the PTI software. Intensity decay curves, $F(t)$, were fitted to multiple exponential decays as:

$$F(t) = \sum_i \alpha_i \cdot e^{-t/\tau_i} \quad (7)$$

where α_i is the preexponential factor (fraction contribution to the time-resolved decay) and τ_i the corresponding lifetime value. Lifetime mean values can be calculated as [27]:

$$<\tau> = \frac{\sum_i^n \alpha_i \tau_i^2}{\sum_i^n \alpha_i \tau_i} \quad (8)$$

3. Results

The characteristics of the liposomes are shown in Table 1. The liposomes mimicking the lipid composition of the HeLa bilayer used for the RBIR experiments were multilamellar vesicles (MLVs) and had an average size of ~ 506 nm after sonication. The large unilamellar vesicles (LUVs) used in the other experiments were similar in diameter (~ 120 nm) after extrusion through the nominal cut-off filter. Polydispersity indices (PDIs) were lower for the LUVs than for the MLVs. On the other hand, the ζ-potentials were quite different in sign. Thus, while HeLa liposomes had a negative charge due to the anionic lipid POPS, the POPC:DOTAP and POPC:CHOL:DOTAP liposomes presented positive values due to the presence of the cationic lipid DOTAP.

HeLa liposome model consisted of three different phospholipids and cholesterol, with the lipid phase of the mixture evaluated by the RBIR methodology. Fig. 1 shows the RBIR values at different temperatures. Linear regression was applied to several portions of the RBIR data. The best fits delimited three regions. After comparing the values obtained in Fig. 1 with those from the study of Sot et al. [13], we assigned the phases for each of the regions. The values of the first region (between 0 and 13 °C), ranging from 0.4 to 0.52, were close to the RBIR values of the membranes in the L_o phase (≈ 0.32), which indicated that the membrane would be in the L_o phase within this region. The values of the last region (between 34 and 55 °C), ranging from 1 to 1.45, were close to those of mixtures in the L_α phase containing cholesterol, such as POPC:CHOL (7:3, mol/mol) and 1,2-dioleoyl-*sn*-glycero-3-phosphocholine DOPC:CHOL (7:3, mol/mol). Thus, above 34 °C, the HeLa-mimicking lipid bilayer would be in the L_α phase. Finally, in the region between 13 and 34 °C, the membrane would be in an intermediate state between those of the L_o and L_α phases. This intermediate state would have intermediate properties between the L_o and L_α phases whose proportions would depend on the specific temperature. That is, it would be closer to the L_o phase at lower temperatures and to the L_α phase at higher temperatures.

We also evaluated the fluidity of the HeLa liposomes by measuring the anisotropic emission of fluorescence, using the DPH or TMA-DPH fluorescent probes. While DPH reports on fluidity at the bilayer core, TMA-DPH, with a net positive charge, reports on the changes near the phospholipid head groups. In these experiments, to compare how the

Table 1
Size, PDI and ζ-potential average values for the liposome formulations.

Liposome composition	Diameter (nm)	PDI	ζ (mV)
HeLa-mimicking LUVs	117.6 ± 1.1	0.122	-8.9 ± 1.1
POPC: DOTAP	120 ± 3	0.194	9.0 ± 1.1
POPC: CHOL: DOTAP	120.7 ± 0.5	0.168	10.1 ± 0.6
HeLa mimicking MLVs (for RBIR)	506 ± 50	0.29	-15.3 ± 0.7

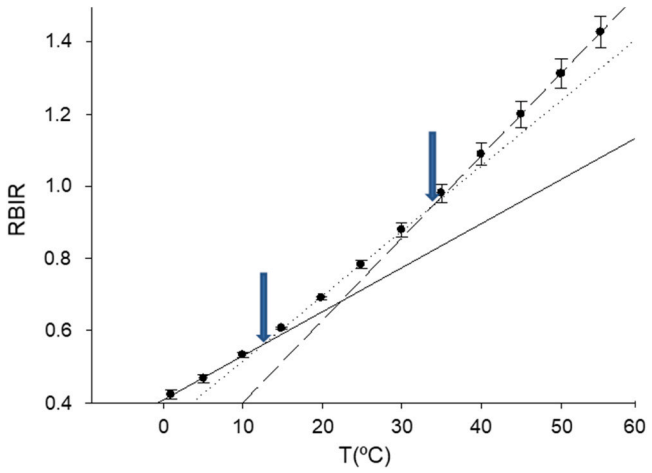

Fig. 1. Red/blue intensity ratio (RBIR) values as a function of temperature of HeLa-mimicking mixture. Linear regression analysis of three groups of experimental data (solid, points and dashed lines), with three delimited regions indicated by the two arrows.

fusion of two vesicle populations influences the microviscosity of the resulting vesicle, we engineered a system with the HeLa-mimicking mixture and the intended fusogenic liposomes at a ratio of 1:1. Fig. 2 shows microviscosity (η), calculated using Eq. 5, as a function of temperature for the three types of liposomes studied. As expected, the η values decreased when the temperature increased for all the lipid compositions studied and for both fluorophores. The microviscosity values of the HeLa liposomes were higher than those of the other two compositions at all the temperatures studied in both regions, showing lower η values in the more hydrophobic region with DPH (Fig. 2A) than in the more hydrophilic region close to the phospholipid head-groups using TMA-DPH (Fig. 2B). When HeLa liposomes were fused with POPC:DOTAP liposomes (dashed lines in Fig. 2), the η values of the sample decreased, especially at lower temperatures. A similar effect was found when POPC:CHOL:DOTAP liposomes were tested for fusion (continuous lines in Fig. 2), although this decrease in the η values was lower than that for the POPC:DOTAP liposomes. Fitting the data from Fig. 2 to Eq. 6 enabled us to obtain ΔE (Table 2). The analysis of the liposome core (DPH) revealed that CHOL in liposomes did not modify the ΔE values, possibly due to its position in the lipid bilayer. On the contrary, the ΔE values obtained with the TMA-DPH probe were of particular interest. While the fusion of the HeLa liposomes with POPC:DOTAP liposomes did not modify the ΔE value, the ΔE value decreased

Table 2
ΔE energy required for flow of DPH and TMA-DPH, and Young's modulus values for HeLa-mimicking liposomes, HeLa-mimicking liposomes with POPC:DOTAP liposomes and HeLa-mimicking liposomes with POPC:CHOL:DOTAP liposomes.

	HeLa-mimicking liposomes		
		+POPC: DOTAP	+POPC: CHOL: DOTAP
ΔE_{DPH} (kJ)	30.8 ± 0.9	34.0 ± 0.7	34.1 ± 0.5
$\Delta E_{TMA\text{-}DPH}$ (kJ)	23.9 ± 0.7	23.6 ± 0.9	22.3 ± 0.7
Young's modulus (MPa)	29.6 ± 0.8	26 ± 5	63.3 ± 0.8
		70.2 ± 1.6	

when incubated with POPC:CHOL:DOTAP liposomes.

Fig. 3 A shows the kinetics of the NBD-PE fluorescence signal in POPC:DOTAP or POPC:CHOL:DOTAP liposomes after the addition of the HeLa liposomes at a ratio of 1:1 ($t = 0$). These results indicated that POPC:CHOL:DOTAP shows higher fluorescence values than POPC:DOTAP, most likely due to the higher dilution of the NBD-PE molecules in the resultant liposome after the fusion process occurred. After one hour of incubation, we used Eq. 2 to calculate the percentage of fusion (Fig. 3B). The fitting of data parameters to Eq. 3 are summarised in Table 3. These values indicated that POPC:CHOL:DOTAP liposomes experienced a more extended degree of fusion (A_{max}), a higher rate of fusion (k) and a large cooperativity value (b) than the POPC:DOTAP liposomes when incubated with the HeLa liposomes.

Furthermore, we evaluated the changes in NBD-PE lifetime according to the lipid composition where it was embedded. Fluorescence lifetime data fitting to Eq.7 is shown in Table S1 (Supplementary Information), while the experimental data are provided in Fig. 4. The average lifetime of NBD-PE was quite similar in the POPC:DOTAP and POPC:CHOL:DOTAP samples, but this decreased when incubated with the HeLa liposomes, notably in the case of POPC:CHOL:DOTAP liposomes.

Fig. 5 shows two AFM images (A and D) of the SLBs obtained by the deposition of HeLa liposomes onto the surface of mica with its corresponding line profiles along the white line (G and J). In both images one can observe that SLBs surfaces are featureless, showing an average height of 4.6 nm ±0.5 nm with respect to the mica (darker areas) and with roughness values (Ra) of 0.45 nm and 0.32 nm, respectively. Fig. 5B was acquired 14 min after the addition of POPC:DOTAP liposomes to the SLB shown in Fig. 5A while Fig. 5C was obtained 30 min after the addition. Both images with Ra values of 0.42 and 0.32 nm, respectively showed similar line profiles (5H and I) where the uncovered mica surface became smaller after the addition of liposomes, indicating

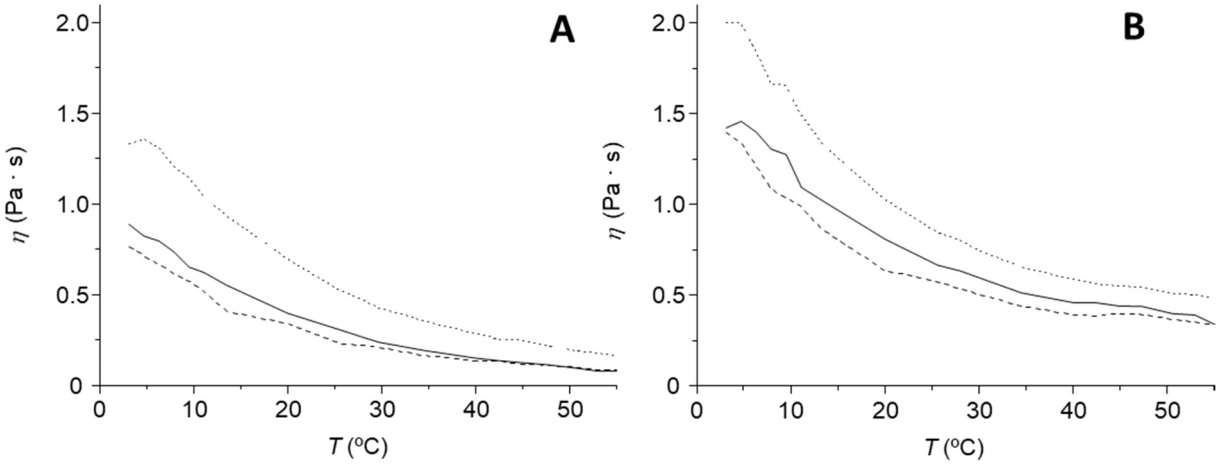

Fig. 2. Microviscosity values (η) and temperature profiles for DPH (A) and TMA-DPH (B) for HeLa-mimicking liposomes before (dotted line) and after the addition of POPC:DOTAP liposomes (dashed line) and POPC:CHOL:DOTAP liposomes (solid line).

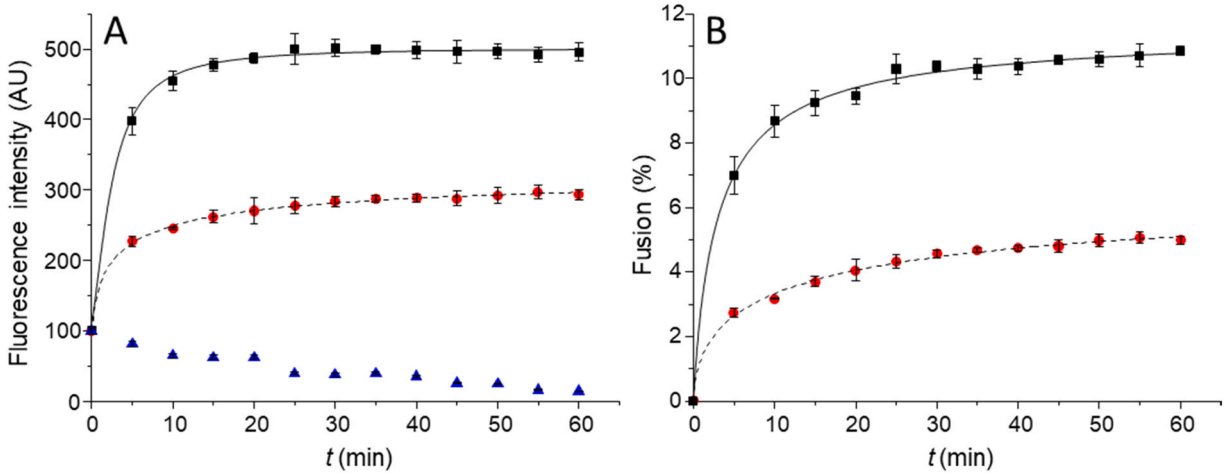

Fig. 3. NBD-PE fluorescence intensity A) and fusion percentage B) as a function of time for HeLa-mimicking liposomes incubated with POPC:DOTAP liposomes (dashed line, circles) and POPC:CHOL:DOTAP liposomes (solid line, squares). Triangles are liposomes without incubation with HeLa-mimicking liposomes (blank).

Table 3
Fitting parameters, A_{max}, k and b, of the fusion ratio as a function of time using Eq. 3.

HeLa-mimicking liposomes +	A_{max}	k (min^{-b})	b	r^2
POPC: DOTAP	7.2 ± 0.9	0.23 ± 0.02	0.60 ± 0.10	0.996
POPC: CHOL: DOTAP	11.4 ± 0.3	0.36 ± 0.06	0.90 ± 0.12	0.997

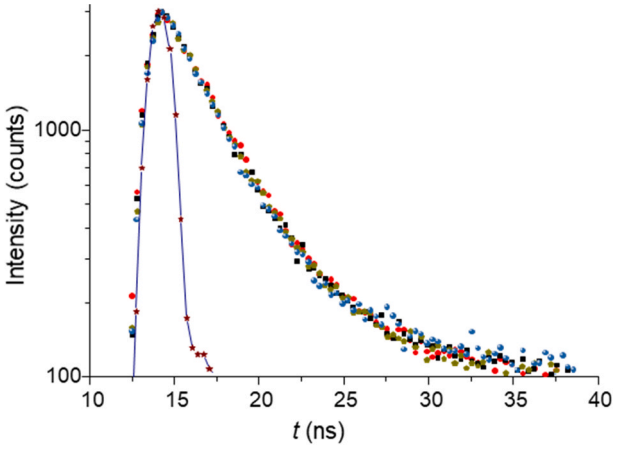

Fig. 4. Fluorescence decay of POPC:DOTAP (Red circles); POPC:CHOL:DOTAP (Black squares); POPC:DOTAP after the addition of HeLa-mimicking liposomes in a ratio of 1:1 (t = 60 min) (Gold pentagons); POPC:CHOL:DOTAP after the addition of HeLa-mimicking liposomes in a ratio of 1:1 (t = 60 min) (Blue spheres) and IRF (Ludox®) (Blue line with brown stars).

that POPC and DOTAP had been integrated into the SLBs. Similarly, 9 min after the addition of POPC:CHOL:DOTAP liposomes to the SLBs previously formed the Hela-mimicking mixture (Fig. 5D), we observed that defects showing bare mica (three small areas) became significantly smaller (Fig. 5E with a *Ra* value of 0.40 nm), to the point that the SLBs covered almost the entire mica surface, as observed after 15 min (Fig. 5F with a *Ra* value of 0.51 nm).

The application of AFM-based force spectroscopy enabled us to calculate the Young's modulus of the SLBs. Fig. 6 shows the histogram-like distribution of the Young's modulus calculated according to Eq. 1 and representative force-curve plots can be found as Supplementary Information (Fig. S1). The adjustment of the distribution to a normal distribution gave a maximum value of 29.6 ± 0.8 MPa for the Young's modulus (Fig. 6A), corresponding to the HeLa-mimicking SLB. The most interesting effect is shown in Fig. 6B, corresponding to the SLB obtained after the addition of POPC:DOTAP liposomes, where two maxima are observed, one centered at 26 ± 5 MPa and the other at 70.2 ± 1.6 MPa. Similar to Fig. 6A, Fig. 6C shows the distribution of the Young's modulus of the SLB resulting from the addition of POPC:CHOL:DOTAP liposomes centered in this case at 63.3 ± 0.8 MPa (Fig. 6C). For clarity, the average Young's modulus values for each system are listed in Table 2.

4. Discussion

The aims of the present work were twofold: (i) to engineer simplified membranes mimicking the lipid composition of the plasma membrane of HeLa cells; and (ii) to assess how they respond to fusion when incubated with liposomes with a defined lipid composition. Such information can be of interest in future works delineated to select lipid liposome composition able to enhance drugs delivery into target cells. Natural membranes, i.e., HeLa cell membrane, present a negative charge due to the presence of phosphatidylglycerol, phosphatidic acid or phosphatidyl inositol groups. Hence, liposomes bearing a positive charge should be electrostatically attracted by the cells. Furthermore, CHOL has been used extensively to promote fusion between lipid vesicles. Thus, we evaluated the fusion of the HeLa-mimicking mixture with liposomes bearing a positive charge, i.e., containing DOTAP lipids, with or without CHOL. In this paper and to this extent, it is worth recalling the value of the zeta potentials of the liposomes investigated. With these effective charges in the bilayers, the primary event occurring in the interaction between the HeLa-mimicking model and the liposomes should be governed by electrostatic forces. Such a mechanism has already been suggested by previous biophysical experiments and also in in vitro experiments using liposomes applied to solid tumours [28]. Remarkably, it has been elsewhere reported that the electrostatic surface event might be the primary step in transfection [29] and viral infection [30]. Moreover, DOTAP appears to cause some structural destabilisation of the bilayer that would precede the fusion process [31].

To evaluate how the HeLa-mimicking bilayer simulated the actual cell lipid bilayer, we analyzed its physicochemical properties by using a planar model (SLBs). In fact, when two vesicles of different sizes come into contact, i.e., eventually HeLa cell and liposomes, the first event would be the adsorption of the smaller system (higher lipid curvature) onto the larger one (low lipid curvature). Therefore, the properties of our flat HeLa SLBs are of interest, especially when a liposome adsorption onto the cell membrane surface or undergoes endocytosis by the cell.

A flat/planar model of the HeLa lipid membrane for AFM

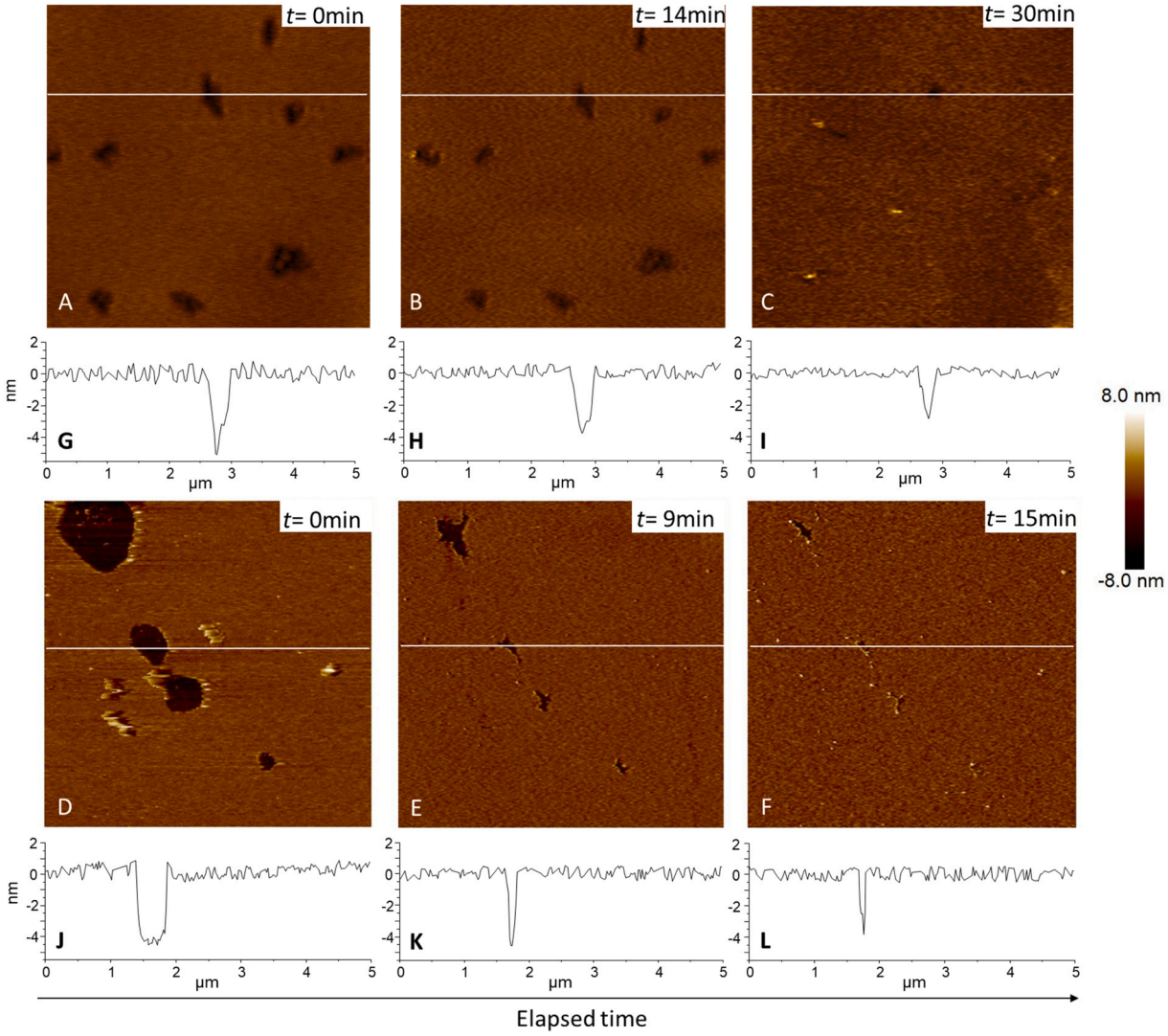

Fig. 5. AFM topographic images of supported lipid bilayers of the HeLa-mimicking mixture before (A, D) and after the addition of POPC:DOTAP liposomes (B and C) and POPC:CHOL:DOTAP liposomes (E and F). Images G-L show the line profiles along the white line in the corresponding upper AFM image.

observations can be obtained by depositing a Langmuir-Blodgett monolayer or by forming a SLBs through the deposition of liposomes onto a mica surface [32]. In a previous study, we observed lipid domains in a HeLa-mimicking monolayer model that seemed to be corroborated the findings of previous Laurdan polarisation and Brewster angle microscopy (BAM) experiments where lipid domains were also observed [12]. Interestingly, in the present work, no laterally segregated domains were observed in the SLBs, suggesting a rearrangement of the lipid components when the liposomes spontaneously adsorbed onto the mica surface. To get a deeper insight into the state of the HeLa-mimicking model we investigated the thermotropic nature of the HeLa liposomes, taking advantage of the PA fluorescent probe [14]. Thus, according to the RBIR values, the liposomes mimicking the HeLa cell lipid membrane, presented an intermediate state between the L_o and L_α phases across the full range of temperatures studied [33]. Fluid states are believed to be preponderant in natural membranes [34], but lateral phase separation, or domains with distinct compositions may exist [35]. However, these domains were not observed by the AFM imaging of the SLBs. Although the RBIR results indicated that the L_o and L_α domains might coexist, we have already reported for POPE and POPE:POPG SLBs that the domains observed in monolayers can disappear when bilayers are formed [36]. If we assume, according to previous BAM observations, that the size of these domains is ~ 10 μm at 30 mN m^{-1} (which is the estimated surface pressure of a bilayer), they fall beyond the scale of the SLB images acquired by AFM in this study. The relationship between coexistence of micro- and nanodomains has been discussed elsewhere [37]. Otherwise, the featureless nature of the HeLa-mimicking SLBs can probably be attributed to the high amount of CHOL (33%) they contain. This observation compares well with other SLB models containing a high proportion of this sterol [38,39].

When POPC:DOTAP liposomes were added to the HeLa SLBs, we observed that they became integrated. Topographic AFM images taken at specific times points did not provide evidence of either vesicular entities adsorbed onto the SLB or reminiscent morphologies of the liposomes. Therefore, the apparent process should probably be attributed to the fusion of the liposomes with preformed SLBs. A similar phenomenon occurred with POPC:CHOL:DOTAP liposomes. Interestingly, when comparing the AFM images acquired for both systems at a similar time point, the results confirmed that the presence of CHOL enhanced the fusion rate. This is in agreement with the results obtained using other techniques investigating the role of CHOL in the fusion process with SLBs of different compositions [40]. The role of CHOL in enhancing membrane fusion has been extensively investigated, but its contribution to the regulation of the process, at least in the presence of other lipids and proteins, remains unknown [41]. We have previously reported that the presence of CHOL increased the fusion of liposomes with monolayers

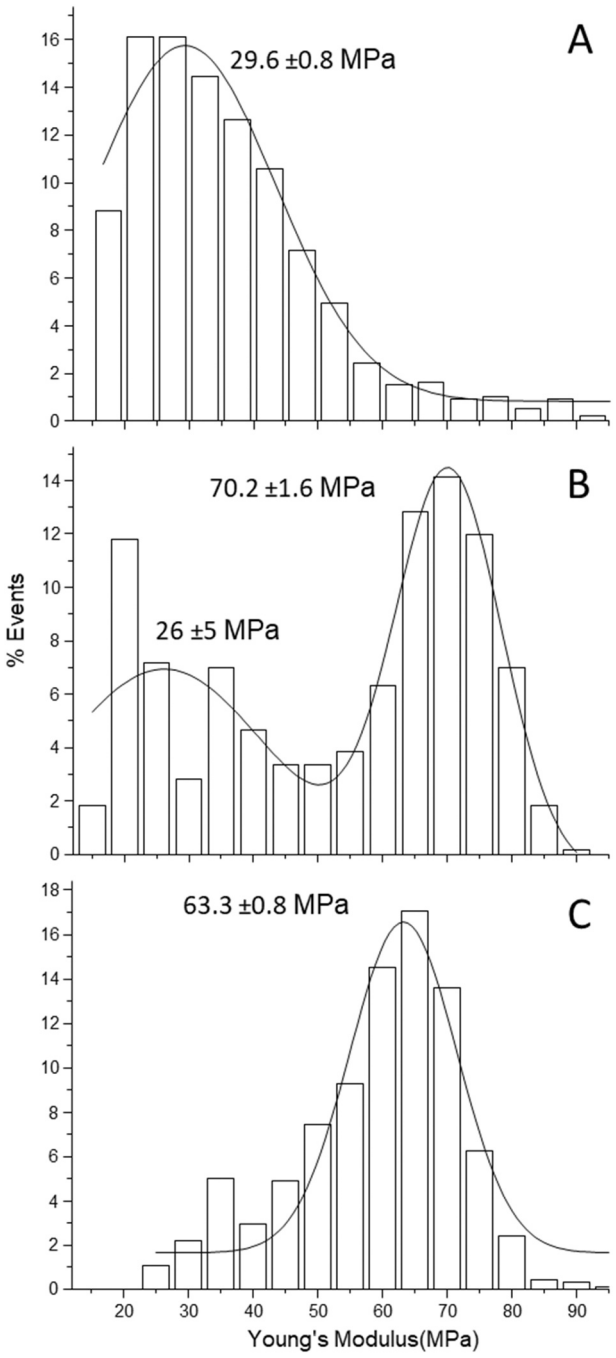

Fig. 6. Young's modulus (E) histograms of HeLa-mimicking bilayer before (A) and after the addition of POPC:DOTAP liposomes (B) and POPC:CHOL:DOTAP liposomes (C). Representational curves are plotted assuming the E distribution fits normal distributions centered in the inset values.

presenting the same composition of that HeLa liposomes used in this work, which agrees with the present AFM observations with liposomes and SLBs.

Analysis of the Young's modulus (*E*) provided further information on the compactness of the SLBs observed with AFM. While high values of *E* correspond to gel or ordered states, low values are typical for fluid or disordered states. For instance, in a well-defined binary phase separated system of 1,2-dioleoyl-*sn*-glycero-3-phosphocholine (DOPC) and 1,2-dipalmitoyl-*sn*-glycero-3-phosphocholine (DPPC), 19.3 MPa and 28.1 MPa have been assigned to the fluid and gel phases, respectively [21]. Even higher values for the same system have been reported when using different AFM probes [42]. From these reference *E* values, our HeLa-mimicking SLB presented an average *E* value of ~ 30 MPa. Therefore, we tentatively propose that the coexistence of the L_o and L_α domains, as predicted by the RBIR measurements, could be displaced towards the L_o phase. However, it is worth noting that for multicomponent SLBs, higher values of up to 80 MPa have been reported for fluid disordered phases [43]. In any case, the increase in the *E* values after incubation with POPC:DOTAP or POPC:CHOL:DOTAP liposomes demonstrates that the flat/planar HeLa-mimicking model is useful for monitoring the fusion of liposomes (high lipid curvature) with a cell membrane (low lipid curvature).

Remarkably, the fusion of liposomes with the HeLa-mimicking flat/planar lipid model membrane resulted in substantial changes in the values and distribution of the Young's modulus. Thus, by fitting the Gaussian model to the experimental results, the unimodal distribution for the HeLa-mimicking SLB becames bimodal when liposomes of POPC:DOTAP were fused, but unimodal and shifting to higher values when POPC:CHOL:DOTAP liposomes were added. Since both types of liposomes contain the same proportion of DOTAP, the positive charge borne by this phospholipid provoked the same repulsion against the AFM tip. Hence, the AFM tip perceived greater repulsion when approaching the lipid and consequently more force was required to deform the surface. The bimodal behaviour observed when adding POPC:DOTAP liposomes could be due to the fact that these components are difficult to integrate or dilute into the SLBs. Therefore, the result would be one region enriched in POPC:DOTAP (which we did not observe in the topographic images by AFM) and with a high Young's modulus value because of the repulsion exerted by DOTAP [44] and another region retaining the elastic properties of the SLB mimicking the HeLa cell lipid membrane. Alternatively, the second peak observed could be due to the DOTAP and the CHOL present in the SLBs interacting in a specific way. In any event, with the addition the POPC:CHOL:DOTAP liposomes, the unimodal distribution shifted towards values slightly lower than that of the second peak observed in the absence of CHOL. These observations are consistent with the reported increase in the bending modulus of liposomes upon the addition of CHOL to different lipid compositions [45] and with seminal works on the nanomechanical properties of SLBs using AFM-based force spectroscopy [46]. As discussed elsewhere, the presence of CHOL in the membrane results in a higher degree of compactness or less elastic deformation of the bilayer [43].

The HeLa-mimicking lipid bilayer model interacted differently with liposomes containing CHOL and those that did not. The results presented in this work, such as the shift towards shorter lifetimes of the NBD-PE fluorescent probe, support the fusion between the bilayers of both types of the liposome formulations studied and the bilayer of the liposomes formed by the HeLa-mimicking composition. As expected, these findings confirmed previous results observed with the monolayer-liposome system, which showed that fusion becomes more extensive in the presence of CHOL [12]. Notice, however, that although the topographic observations made with AFM could call into question the temporal resolution of the technique, the FRET results confirmed that the fusion process was faster in the presence of CHOL, as depicted by the kinetic constant values (Table 3), being ~ 40% higher in the presence of the sterol. Although the fusion percentage did not reach high values (11.4% and 7.2% for the POPC:CHOL:DOTAP and POPC:DOTAP liposomes, respectively), it is worth mentioning here that the maximum fusion values were calculated by considering that all the liposomes bearing the fluorescent dyes were infinitely diluted, i.e., disrupting liposomes with detergents. Instead, by considering that all the liposomes bearing fluorescent probes fused with all the liposomes of the HeLa-mimicking mixture, the maximum percentage of fusion was calculated to be 42.1% and 18.1% for the POPC:CHOL:DOTAP and POPC:DOTAP liposomes, respectively. (Fig. S2 and Table S2 in the Supplementary Information).

HeLa liposomes showed more viscosity before than after fusion with the different liposomes studied. The decrease in viscosity was greater

after fusion with the POPC:DOTAP liposomes than after fusion with the POPC:CHOL:DOTAP liposomes. Since both liposomes contain the same molar proportion of DOTAP (20%), the structural destabilisation caused by the positive phospholipid [47] results in lower values of micro-viscosity. However, the presence of CHOL in the liposomes increases viscosity by causing an ordering effect in the membrane [48]. The changes in viscosity of the HeLa-mimicking liposomes during fusion with liposomes demonstrate that the composition of the bilayer changes due to the fusion and consequent insertion of the molecules from the engineered liposomes. Furthermore, the ΔE values extracted from the microviscosity measurements could be interpreted, in a comparative manner, as an indicator of the ease with which liposomes extend onto a surface. However, no major differences were observed when using either DPH or TMA-DPH, indicating that both types of liposomes require a similar amount of energy to promote the fusion mechanisms.

5. Conclusions

The HeLa bilayer lipid model formed by four phospholipids (POPC: POPE:POPS:CHOL) is able to form liposomes and SLBs after deposition onto mica. Because of the high proportion of CHOL, HeLa liposomes present an equilibrium between L_o and L_α phases, according to RBIR measurements. AFM observations have shown flat and featureless SLBs with no evidence of lateral segregation in either phase. POPC:DOTAP and POPC:CHOL:DOTAP liposomes are able to integrate into the pre-formed HeLa SLBs, suggesting the existence of a fusion process as the SLBs expand covering the empty areas of the substrate. From AFM force spectroscopy assays, it is observed that the stiffness of the membrane varies because of the integration in the SLBs of the lipids supplied by the liposomes. We also observed by means of fluorescence lifetime experiments, that the mean decay lifetime is also affected in the resultant liposome. We have positively confirmed the fusion mechanism by incubating HeLa liposomes with POPC:DOTAP or POPC:CHOL:DOTAP liposomes using FRET assays. While the presence of CHOL increases the Young's modulus of the resultant SLBs, FRET experiments confirm that CHOL enhances the fusion mechanism. The changes in microviscosity confirm the integration of the lipids from the liposomes within the HeLa-mimicking lipid model. It is important to emphasise here that stiffness and viscosity values obtained from Young's modulus (AFM) and from fluorescence (DPH and TMA-DPH probes) are not contradictory but complementary. While from the Young's modulus data we obtain information on the compactness between phospholipids, the amount of force applied in the Z axis needed to separate them, and the increase of the Young's modulus value demonstrates the changes in the composition of the resultant SLBs. Finally, viscosity data obtained from anisotropy of TMA-DPH probe provide information on the mobility of the lipids in the XY plane suggesting that the presence of CHOL decreases the activation energy.

By assessing two simplified Hela-mimicking lipid model membranes in the fusion process with two types of liposomes bearing CHOL and/or a positive charge we have undertaken a new research project aiming to use these lipid compositions to evaluate how the lipid composition of the HeLa plasma membrane could be the responsible of the delivery and internalization of encapsulated substances into the intracellular liquid medium. We are presently undertaken a project that is directed to bring light, from a biophysical point of view, on how genes and/or proteins can be delivered into living HeLa cell membranes. One of the strategies contemplates the use of fusion peptides integrated into the liposome bilayer with the goal of facilitating liposome-cell recognition.

Outcoming results outcoming from this new project will be present in a following paper.

CRediT authorship contribution statement

A. Botet-Carreras: Investigation, Formal analysis, Writing – original draft; M.T. Montero: Conceptualization, Visualization, Writing – reviewing & editing; J. Sot: Investigation, Formal analysis, Writing – reviewing & editing; Ò. Domènech: Formal analysis, Supervision, Writing – reviewing & editing; J.H. Borrell: Conceptualization, Supervision, Writing – reviewing & editing.

Declaration of Competing Interest

The authors declare the following financial interests/personal relationships which may be considered as potential competing interests: Jordi H. Borrell reports equipment, drugs, or supplies was provided by Spanish Ministry of Economy and Competitiveness (PID2019-110210GB-I00) and the Catalan Government (Generalitat de Catalunya) (214SGR 1442). Oscar Domenech reports equipment, drugs, or supplies was provided by Spanish Ministry of Economy and Competitiveness (PID2019-110210GB-I00) and the Catalan Government (Generalitat de Catalunya) (214SGR 1442). M. Teresa Montero reports equipment, drugs, or supplies was provided by Spanish Ministry of Economy and Competitiveness (PID2019-110210GB-I00) and the Catalan Government (Generalitat de Catalunya) (214SGR 1442). Jesus Sot reports equipment, drugs, or supplies was provided by Basque Government (IT1264-19 and IT1270-19).

Acknowledgements

This study was supported by the Spanish Ministry of Economy and Competitiveness (PID2019-110210GB-I00), the Catalan Government (*Generalitat de Catalunya*) (214SGR 1442), the Basque Government (grants No. IT1264-19 and IT1270-19), the Fundación Biofísica Bizkaia and the Basque Excellence Research Centre (BERC). We thank Andrey Klymchenko (Laboratoire de Bioimagerie et Pathologies, UMR 7021 CNRS, Faculté de Pharmacie, Université de Strasbourg, 67401 Illkirch, France) for the generous gift of PA. Special thanks to Dr Felix M. Goñi and Dr Manuel Prieto for their comments and suggestions. The authors want to thank Dr Pawel Wydro for hosting A. B-C. in his lab during a short stay and Dr Christopher Evans for English language revision.

Appendix A. Supporting information

Supplementary data associated with this article can be found in the online version at doi:10.1016/j.colsurfa.2021.127663.

References

[1] Q. Guo, C. Jiang, Delivery strategies for macromolecular drugs in cancer therapy, Acta Pharm. Sin. B 10 (2020) 979–986.
[2] N. Azad, Y. Rojanasakul, Macromolecular drug delivery. Biopharm. Drug Des. Dev., Humana Press, Totowa, NJ, 2008, pp. 293–323.
[3] R. Zhang, X. Qin, F. Kong, P. Chen, G. Pan, Improving cellular uptake of therapeutic entities through interaction with components of cell membrane, Drug Deliv. 26 (2019) 328–342.
[4] M. Riaz, M. Riaz, X. Zhang, C. Lin, K. Wong, X. Chen, G. Zhang, A. Lu, Z. Yang, Surface functionalization and targeting strategies of liposomes in solid tumor therapy: a review, Int. J. Mol. Sci. 19 (2018) 195.
[5] J.E. Rothman, The principle of membrane fusion in the cell (Nobel Lecture), in: Angew. Chemie Int. Ed, 53, 2014, pp. 12676–12694.
[6] C. Hamai, T. Yang, S. Kataoka, P.S. Cremer, S.M. Musser, Effect of average phospholipid curvature on supported bilayer formation on glass by vesicle fusion, Biophys. J. 90 (2006) 1241–1248.
[7] R. Kolašinac, S. Jaksch, G. Dreissen, A. Braeutigam, R. Merkel, A. Csiszár, Influence of environmental conditions on the fusion of cationic liposomes with living mammalian cells, Nanomaterials 9 (2019) 1025.
[8] R. Rahbari, T. Sheahan, V. Modes, P. Collier, C. Macfarlane, R.M. Badge, A novel L1 retrotransposon marker for HeLa cell line identification, Biotechniques 46 (2009) 277–284.
[9] W. Barcellini, P. Bianchi, E. Fermo, F.G. Imperiali, A.P. Marcello, C. Vercellati, A. Zaninoni, A. Zanella, Hereditary red cell membrane defects: diagnostic and clinical aspects, Blood Transfus. 9 (2011) 274–277.
[10] WHO Human Genetics Programme, The molecular genetic epidemiology of cystic fibrosis: report of a joint meeting of WHO/IECFTN/ICF(↱M)↱A/ECFS, World Heal. Organ. (2004) 1–24.
[11] C.A. Hubner, Ion channel diseases, Hum. Mol. Genet. 11 (2002) 2435–2445.

[12] A. Botet-Carreras, M.T. Montero, J. Sot, Ò. Domènech, J.H. Borrell, Characterization of monolayers and liposomes that mimic lipid composition of HeLa cells, Colloids Surf. B 196 (2020), 111288.
[13] J. Sot, I. Esnal, B.G. Monasterio, R. León-Irra, Y. Niko, F.M. Goñi, A. Klymchenko, A. Alonso, Phase-selective staining of model and cell membranes, lipid droplets and lipoproteins with fluorescent solvatochromic pyrene probes, BBA-Biomembr. 2021 (1863), 183470.
[14] Y. Niko, S. Kawauchi, G. Konishi, Solvatochromic pyrene analogues of prodan exhibiting extremely high fluorescence quantum yields in apolar and polar solvents, Chem. -Eur. J. 19 (2013) 9760–9765.
[15] X. Li, Y.-J. Yuan, Lipidomic analysis of apoptotic Hela cells induced by paclitaxel, Omi. A J. Integr. Biol. 15 (2011) 655–664.
[16] M.L. Torgersen, T.I. Klokk, S. Kavaliauskiene, C. Klose, K. Simons, T. Skotland, K. Sandvig, The anti-tumor drug 2-hydroxyoleic acid (Minerval) stimulates signaling and retrograde transport, Oncotarget 7 (2016) 86871–86888.
[17] M.J. Gerl, V. Bittl, S. Kirchner, T. Sachsenheimer, H.L. Brunner, C. Lüchtenborg, C. Özbalci, H. Wiedemann, S. Wegehingel, W. Nickel, P. Haberkant, C. Schultz, M. Krüger, B. Brügger, Sphingosine-1-phosphate lyase deficient cells as a tool to study protein lipid interactions, PLoS One 11 (2016), e0153009.
[18] M. Lorizate, T. Sachsenheimer, B. Glass, A. Habermann, M.J. Gerl, H.-G. Kräusslich, B. Brügger, Comparative lipidomics analysis of HIV-1 particles and their producer cell membrane in different cell lines, Cell. Microbiol 15 (2013) 292–304.
[19] C. Suárez-Germà, M.T. Montero, J. Ignés-Mullol, J. Hernández-Borrell, Ò. Domènech, Acyl chain differences in phosphatidylethanolamine determine domain formation and LacY distribution in biomimetic model membranes, J. Phys. Chem. B 115 (2011) 12778–12784.
[20] J.J. Roa, G. Oncins, J. Diaz, F. Sanz, M. Segarra, Calculation of Young's modulus value by means of AFM, Recent Pat. Nanotechnol. 5 (2011) 27–36.
[21] L. Picas, F. Rico, S. Scheuring, Direct measurement of the mechanical properties of lipid phases in supported bilayers, Biophys. J. 102 (2012) L01–L03.
[22] D.K. Struck, D. Hoekstra, R.E. Pagano, Use of resonance energy transfer to monitor membrane fusion, Biochemistry 20 (1981) 4093–4099.
[23] C. François-Martin, F. Pincet, Actual fusion efficiency in the lipid mixing assay - comparison between nanodiscs and liposomes, Sci. Rep. 7 (2017) 43860.
[24] S. Merino-Montero, M.T. Montero, J. Hernández-Borrell, Effects of lactose permease of Escherichia coli on the anisotropy and electrostatic surface potential of liposomes, Biophys. Chem. 119 (2006) 101–105.
[25] M. Shinitzky, Y. Barenholz, Fluidity parameters of lipid regions determined by fluorescence polarization, BBA-Biomembr. 515 (1978) 367–394.
[26] T. Kure, H. Sakai, Transmembrane difference in colloid osmotic pressure affects the lipid membrane fluidity of liposomes encapsulating a concentrated protein solution, Langmuir 33 (2017) 1533–1540.
[27] J.R. Lakowicz, Measurement of fluorescence lifetimes, in: Princ. Fluoresc. Spectrosc., Springer US, Boston, MA, 1983, pp. 51–93.
[28] S. Krasnici, A. Werner, M.E. Eichhorn, M. Schmitt-Sody, S.A. Pahernik, B. Sauer, B. Schulze, M. Teifel, U. Michaelis, K. Naujoks, M. Dellian, Effect of the surface charge of liposomes on their uptake by angiogenic tumor vessels, Int. J. Cancer 105 (2003) 561–567.
[29] D. Simberg, S. Weisman, Y. Talmon, Y. Barenholz, DOTAP (and other cationic lipids): chemistry, biophysics, and transfection, Crit. Rev. Ther. Drug 21 (2004) 257–317.
[30] S.C. Harrison, Viral membrane fusion, Virology 479–480 (2015) 498–507.
[31] R. Guo, Y. Liu, K. Li, B. Tian, W. Li, S. Niu, W. Hong, Direct interactions between cationic liposomes and bacterial cells ameliorate the systemic treatment of invasive multidrug-resistant Staphylococcus aureus infections, Nanomed. Nanotechnol. 34 (2021), 102382.
[32] L. Picas, P.-E. Milhiet, J. Hernández-Borrell, Atomic force microscopy: a versatile tool to probe the physical and chemical properties of supported membranes at the nanoscale, Chem. Phys. Lipids 165 (2012) 845–860.
[33] G. van Meer, D.R. Voelker, G.W. Feigenson, Membrane lipids: where they are and how they behave, Nat. Rev. Mol. Cell Biol. 9 (2008) 112–124.
[34] M.D. Houslay, K.K. Stanley, Dynamics of Biological Membranes, John & Wiley Sons,, Chischester, 1983.
[35] T. Baumgart, S.T. Hess, W.W. Webb, Imaging coexisting fluid domains in biomembrane models coupling curvature and line tension, Nature 425 (2003) 821–824.
[36] L. Picas, C. Suárez-Germà, M. Teresa Montero, J. Hernández-Borrell, Force spectroscopy study of Langmuir−Blodgett asymmetric bilayers of phosphatidylethanolamine and phosphatidylglycerol, J. Phys. Chem. B 114 (2010) 3543–3549.
[37] Ò. Domènech, J. Ignés-Mullol, M.T. Montero, J. Hernandez-Borrell, Unveiling a complex phase transition in monolayers of a phospholipid from the annular region of transmembrane proteins, J. Phys. Chem. B. 111 (2007) 10946–10951.
[38] L. Redondo-Morata, M.I. Giannotti, F. Sanz, Influence of cholesterol on the phase transition of lipid bilayers: a temperature-controlled force spectroscopy study, Langmuir 28 (2012) 12851–12860.
[39] Z. Al-Rekabi, S. Contera, Multifrequency AFM reveals lipid membrane mechanical properties and the effect of cholesterol in modulating viscoelasticity, Proc. Natl. Acad. Sci. 115 (2018) 2658–2663.
[40] D.E. Lee, M.G. Lew, D.J. Woodbury, Vesicle fusion to planar membranes is enhanced by cholesterol and low temperature, Chem. Phys. Lipids 166 (2013) 45–54.
[41] S.-T. Yang, A.J.B. Kreutzberger, J. Lee, V. Kiessling, L.K. Tamm, The role of cholesterol in membrane fusion, Chem. Phys. Lipids 199 (2016) 136–143.
[42] O. Saavedra V, T.F.D. Fernandes, P.-E. Milhiet, L. Costa, Compression, rupture, and puncture of model membranes at the molecular Scale, Langmuir 36 (2020) 5709–5716.
[43] R.M. a Sullan, J.K. Li, S. Zou, Direct correlation of structures and nanomechanical properties of multicomponent lipid bilayers, Langmuir 25 (2009) 7471–7477.
[44] M. N'Diaye, J.-P. Michel, V. Rosilio, Relevance of charges and polymer mechanical stiffness in the mechanism and kinetics of formation of liponanoparticles probed by the supported bilayer model approach, Phys. Chem. Chem. Phys. 21 (2019) 4306–4319.
[45] Y. Takechi-Haraya, K. Sakai-Kato, Y. Abe, T. Kawanishi, H. Okuda, Y. Goda, Atomic force microscopic analysis of the effect of lipid composition on liposome membrane rigidity, Langmuir 32 (2016) 6074–6082.
[46] S. Garcia-Manyes, L. Redondo-Morata, G. Oncins, F. Sanz, Nanomechanics of lipid bilayers: heads or tails? J. Am. Chem. Soc. 132 (2010) 12874–12886.
[47] N. Benne, R.J.T. Leboux, M. Glandrup, J. van Duijn, F. Lozano Vigario, M. A. Neustrup, S. Romeijn, F. Galli, J. Kuiper, W. Jiskoot, B. Slütter, Atomic force microscopy measurements of anionic liposomes reveal the effect of liposomal rigidity on antigen-specific regulatory T cell responses, J. Control. Release 318 (2020) 246–255.
[48] T. Róg, M. Pasenkiewicz-Gierula, I. Vattulainen, M. Karttunen, Ordering effects of cholesterol and its analogues, BBA-Biomembr. 2009 (1788) 97–121.